Climate Data Record (CDR) Program

Climate Algorithm Theoretical Basis Document (C-ATBD)

Daily 1/4° Optimum Interpolation Sea Surface Temperature (OISST)

REVISION HISTORY

Rev.	Author	DSR No.	Description	Date
1	Viva Banzon	DSR-340	Initial Submission to CDR Program	07/10/2013

TABLE of CONTENTS

LIST of FIGURES

LIST of TABLES

1.   Introduction

1.1   Purpose

The purpose of this document is to describe the algorithm for the sea surface temperature (SST) analysis known as the Daily ¼° Optimum Interpolation SST (OISST) Climate Data Record (CDR), that has been submitted to the National Climatic Data Center (NCDC) by Richard W. Reynolds and Viva Banzon. This document describes the version 2 (or v2) algorithm but much of the material is derived from Reynolds et al. (2007) that introduced the original version 1 (or v1). The main changes from v1 to v2 are listed in Table 1 but more details can be found in Reynolds (2008). The daily OISST uses satellite data from the Advanced Very High Resolution Radiometer (AVHRR), an infrared instrument, which has been providing SST observations since late 1981. AVHRR has been flown on a series of NOAA satellites, but more recently, also on European METeorologial OPeration (or METOP) satellites. The daily OISST algorithm is implemented in the computer program (code) that accompanies this document, and thus the intent here is to provide a guide to understanding that algorithm, from both a scientific perspective and in order to assist a software engineer or end-user performing an evaluation of the code.

Unlike most other thematic CDRs that are geophysical parameters derived from satellite data using an algorithm, this product is made by blending SST data from different source types. An analysis puts irregularly spaced SST observations on a regular grid and applies statistical techniques to fill in gaps. Because this SST analysis is designed for climate research, it has reduced spatial and temporal resolution relative to the input data in order to reduce sampling error. There are several optimally interpolated SST products in circulation referred to as OISST. This document provides details only for the daily ¼° OISST. Moreover, this CATBD describes the "AVHRR-only" product which uses AVHRR observations from late 1981 to the present.

The daily OISSTv2 is also available as an "AVHRR+AMSR" analysis for the 2002 to 2011 period, but is not described in this document. "AVHRR+AMSR" is similar to "AVHRR-only" except that it includes additional data from the Advanced Microwave Scanning Radiometer on the EOS platform (AMSR-E). AMSR-E now has degraded capabilities, and WindSat has been identified as an alternative source of microwave SSTs for the daily OISST (Banzon and Reynolds 2013). The routine AVHRR+AMSR production may be restarted with the release of the next generation AMSR2 SST data in 2013. The methods presented in this document can be applied to both products, but the inputs will differ between products.

1.2   Definitions

Following is a summary of the symbols used to define the OI algorithm.

Optimum Interpolation (OI) parameters: The index i is used for data type (e.g., daily ship, daily buoy, AVHRR daytime, AVHRR nighttime) while k is used for the analysis grid points. Normally, q and r are differences with respect to a first guess

reference system. This difference is sometimes referred to as an "increment". For this product, the first guess is the analysis from the previous day.

$$r_k = \text{ analyzed SST (°C) at grid point } k \tag{1}$$

$$q_i = \text{ SST data (°C) of type } i \tag{2}$$

$$N = \text{ number of SST data values} \tag{3}$$

$$w_{ik} = \text{OI linear weights determined by regression} \tag{4}$$

1.3   Document Maintenance

This document describes the initial submission version of the processing algorithm and resulting data. The document version number will be incremented for any subsequent enhancements or revisions.

2.   Observing Systems Overview

2.1   Products Generated

The daily OISSTv2 is a global SST analysis at ¼ ° spatial grid resolution and 1-day temporal resolution, from September 1981 to the present. The netCDF files described here are archived at NCDC and available at the product website http://www.ncdc.noaa.gov/oa/climate/research/sst/oi-daily-information.php. The analyzed SST in (°C) is the core CDR product, but the netCDF file also contains three other fields: the SST anomaly (i.e., difference with respect to 1971-2000 climatology, also in °C), the analysis total error (i.e., standard deviation; see 3.4.4) in °C, and the median sea ice concentrations, expressed as fraction of the total area, ranging from 0 to 1 to represent none to 100% sea ice cover. The anomalies are provided to facilitate climate applications such as computation of El Nino indices. The total error provides a measure of confidence associated with each grid estimate. The median sea ice is a processing by-product (described in section 3.3.3), used to estimate ocean temperatures at the sea-ice edge, and is included to allow checking when an unrealistic proxy SST value occurs. A satellite with drifting calibration can result in bad ice values. The ice field should not be used for other purposes such as monitoring or modeling.

More recent SST product standards and formats have been developed by the Group for High Resolution Sea Surface Temperature (GHRSST). Thus, the OISST code also produces another netCDF file that conforms to GHRSST Data Specifications (https://www.ghrsst.org/documents/q/category/gds-documents/operational/). The GHRSST-compliant netCDF file is sent to Jet Propulsion Laboratory (NASA) which is a designated GHRSST Global Data Assembly Center and archived at NOAA's National Oceanographic Data Center (NODC), the designated GHRSST Long-term Stewardship Facility.

2.2   Instrument Characteristics

The OISST code does not perform any satellite retrievals. Satellite inputs (i.e., AVHRR SSTs and the microwave sea ice concentrations) come from external providers that perform the task of deriving geophysical parameters from raw sensor data. Links to instrument descriptions are provided here only for completeness.

AVHRR technical documentation (e.g., instrument, operational data formats) is available online at http://www.ncdc.noaa.gov/oa/pod-guide/ncdc/docs/intro.htm. The NOAA Polar Orbiter Data User's Guides (PODUG) November 1998 revision describes NOAA14 and earlier, while the next generation instruments covering NOAA15 and later are covered by the NOAA KLM User's Guide (April 2009 revision). NOAA-N (NOAA19 after launch) and -P are also described in the NOAA-N,-P Supplement http://www.ncdc.noaa.gov/oa/pod-guide/ncdc/docs/klm/nnpsupp.htm

Sea ice concentrations are derived from microwave data collected by instruments flown primarily on the Defense Meteorological Satellite program (DMSP) satellites. These include the Scanning Multichannel Microwave Radiometer (SSMR), the

Special Sensor Microwave Imager (SSMI), and the Special Sensor Microwave Imager/Sounder (SSMI/S). Details on instruments and ice concentration algorithms can be found in CDR documents (http://www1.ncdc.noaa.gov/pub/data/sds/cdr/docs/sea-ice-concentration-catbd.pdf; http://www1.ncdc.noaa.gov/pub/data/sds/cdr/docs/rss-v6.0-ssmi-fcdr-catbd.pdf). The Remote Sensing Systems webpages (http://www.remss/com/) also provide information and data from many microwave sensors. As described in 3.3.1, a gap in SSMI data from May 2009 to October 2011 was covered using AMSR-E (http://www.ghcc.msfc.nasa.gov/AMSR/instrument_descrip.html).

3.   Algorithm Description

3.1   Algorithm Overview

Section 3 describes the OISST.v2 algorithm. Note that the scripts submitted are only for routine forward processing (sometimes also referred to as operations), but the principles are similar for the retrospective (or historical) period. Both use the same core programs. A processing flow overview is given in Section 3.2. Section 3.3 describes the input datasets (satellite SSTs, in situ SSTs, and satellite ice concentrations), as well as ancillary files. The theoretical background and computations are discussed in Section 3.4.
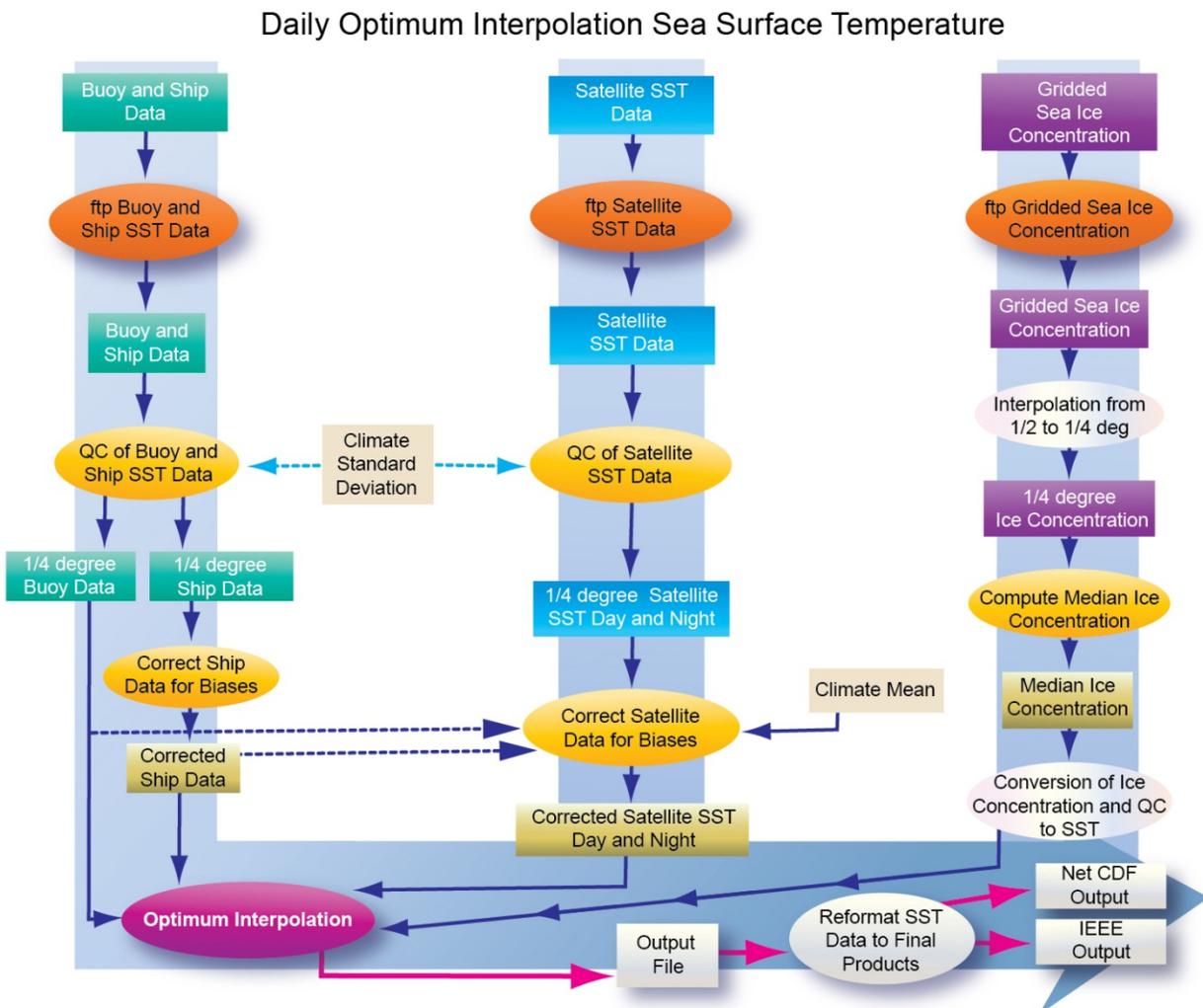
3.2   Processing Outline

Figure 1: OISST Routine Processing flow. Not all ancillary data are shown

       Routine production flow is shown in Fig. 1. Near-real time inputs are downloaded and prepared prior to the interpolation. The chart shows three paths corresponding to the preparation of each input type: 1) satellite-derived temperatures, 2) in situ SSTs from ships and buoys, and 3) sea ice concentrations. The ultimate goal of each path is to put all SST inputs on a ¼° grid. Observations from in situ platforms (ship and buoy separately) are averaged onto the ¼° grid to form superobservations.   The ship data are bias-adjusted to the buoys. The in situ superobservations (bias-adjusted ship and unadjusted buoy) are then collectively used to correct the satellite data (nighttime and daytime separately), also gridded to ¼°. The ice preparation is completely independent of the other two. Sea ice concentrations are gridded to ¼°, smoothed, and then converted to proxy SSTs. When preparation of the three datasets is complete, they are combined and interpolated to produce a gap-free SST product.   Files are written in binary but the analysis results are also converted to netCDF.

Table 1: Comparison of OISST versions. The interim run is also referred to as preliminary or near real time. Large scale bias corrections are made to satellite data using Empirical Orthogonal Teleconnections (EOT) modes (section 3.4). Zonal corrections primarily vary by latitude, and are used only if EOT corrections cannot be made due to lack of in situ data.

OISST feature	V1	Interim V2	Final V2
Time delay	1 day	1 day	14 days
Days of data used in OI	1	1	3
Ship Bias correction	No	Yes	Yes
Zonal Bias Correction	No	Yes	Yes
Smoothing of EOT modes	No	No	5 days
Days of in situ data in EOT bias correction	7 days	7 days	15 days
Start of AVHRR-only QDOISST time series	Jan 1985	(replaced by final)	Sep 1981

       In practice, the routine processing of a single day's data is performed twice, with a lag of 1 and 14 days, to produce a preliminary (also called "interim" or "near real time") and a "final" product, respectively. The difference between the two runs is listed in Table 1. The processing features are explained in detail in section 3.4. Redundant steps are skipped the second time around. The "interim" run uses less days of data. After 2 weeks, the "final" version is made using additional or updated data. It should be noted that aside from the difference in input data, the "final" is identical to the retrospective processing. The preliminary OISST is not archived at NCDC and not submitted as a CDR since it is a poorer quality product. However, the GHRSST archive process may save the preliminary netCDF which can be easily identified by the word "interim" (as opposed to "final") in the metadata.

3.3   Algorithm Input

3.3.1   Primary Input Data

Satellite SST. From 2007 onward, the operational Navy AVHRR SSTs (May et al. 2001) are used in OISST. The Naval Oceanographic Office located at the Stennis Space Center Mississippi is the Core Processing Center for Global Sea Surface Temperature under the NOAA/DOD Shared Processing Program, established in 1978. The 6-hourly Navy AVHRR SST data are downloaded from the NOAA/NESDIS Data Distribution System (ftp://dds.nesdis.noaa.gov; registration required). The filename is of the form navysst.tmpobs.n19m02n18.yyyyddd.hh, where "n19m02n18" specifies the source satellites. That is, the file contains separate SST records from each operational NOAA satellite, and the user can select which sensors to use. Weekly aggregates of the 6-hourly data are archived (see KLM POD guide). Routine OISST production uses two operational AVHRRs (e.g., in 2012, NOAA 19 and METOP-A). The AVHRR data is quality screened and superobservations are formed on a ¼° grid, producing two global fields (night- and daytime) separately for each satellite.

When the daily OISST v2 was released, Pathfinder Sea Surface temperature (PFSST) data (version 5.0/5.1) was available only up to 2007. For the daily OISST, PFSSTs were used when possible because PFSSTs have been shown to be are more consistent with in situ data than the operational Navy SSTs (Reynolds et al. 2007). A new PFSST version 5.2 (also a CDR) is now available in netCDF but the daily OISST code needs to be updated to accommodate changes in the PFSST resolution and format. The older PFSST v5.0/5.1 are available at NODC (http://www.nodc.noaa.gov/SatelliteData/pathfinder4km/) on a 4.9 km global grid (separate daytime and nighttime) and are written in HDF format. PFSST v5.0 covers the 1985 to 2005 period. PFSST code was upgraded to v5.1 to be able to process NOAA7 data from 1981 to early 1985. The PFSST time series uses a single (the most reliable) AVHRR at any one time, so the retrospective processing is based on one satellite unlike the routine processing that uses Navy SSTs from two satellites. Aside from this difference, the data preparation is identical to routine processing.

In situ SST. SST observations from ships and buoys (moored and drifting) are relayed via the Global Telecommunications System (GTS) in near real time. A daily in situ data file called gts.1day.dat.gz at ftp://ftp.emc.ncep.noaa.gov/cmb/misc/rwr/ is provided by special arrangement with Diane Stokes at the National Centers for Environmental Prediction (NCEP). This file is replaced every day. Data from previous days are aggregated in a monthly file for the past (called gts.sfcmar.gz) or current month (gts.sfcmar.partial.gz), available at ftp://ftp.emc.ncep.noaa.gov/cmb/obs/gts/. Until Feb 2011, these near real time monthly were posted at the Earth System Research Laboratory website (http://icoads.noaa.gov/nrt.html).

The International Comprehensive Ocean–Atmosphere Dataset (ICOADS: e.g., Woodruff et al. 2011) provides SST observations for the historical period, as well as monthly updates. For OISSTv2, an earlier version of ICOADS was used, but ICOADS 2.5 is the latest release. Orders for specific time periods, variables and fields can be made at http://rda.ucar.edu/datasets/ds540.0/. The historical observations are rewritten as daily files, separately for ships and buoys. These daily observations are then quality screened, and averaged onto the ¼° grid to form ship and buoy super-observations.

Most ship observations in the 1981–2006 period were made from insulated buckets, hull contact sensors, and engine condenser intakes at depths of one to several meters. Although selected SST observations can be very accurate (see Kent et al. 1999; Kent and Taylor 2006), typical rms errors of individual observations from ships are larger than 1°C and may have biases of a few tenths of a degree Celsius. SST observations from drifting and moored buoys are typically made by a thermistor or hull contact sensor and usually are transmitted in real time via satellite. Although the accuracy of the buoy SST observations varies, the random error is usually smaller than 0.5°C, which is significantly smaller than ship SST errors. Thus, the gridded buoy fields are not bias adjusted, while a constant (0.14 °C) is removed from the ship superobservations. This constant was obtained by linear regression of co-located monthly averages of ship and buoy anomalies (see section 3.4.6; Reynolds et al. 2010; Reynolds 2008).

Sea ice concentrations. In situ and satellite observations tend to be sparse in the marginal ice zone. Thus, sea ice concentration data are used to obtain proxy estimates of SST. The conversion to SST is discussed in section 3.3.3. The NCEP real-time sea ice product (1/2° grid; GRIB format) described in Grumbine (1996) is used from 2005 to the present. The Grumbine product uses data gathered from different sensors and has not been reanalyzed to produce a consistent long-term dataset (see Reynolds et al. 2007). Sensor and algorithm changes, as well as the consequent impact on the temporal consistency, are noted at the website http://polar.ncep.noaa.gov/seaice/Analyses.html where the data can be obtained. The producer (robert.grumbine@noaa.gov) can be contacted directly.

Delayed sea ice concentrations (NASA Team algorithm; Cavalieri et al., 1999) are used for the 1981 to 2004 period. At the time of the OISSTv2 release, the reprocessed ice was available only until 2004 but since then, this dataset has been extended. The Cavalieri product is distributed (in polar stereographic projection; IEEE format) by the National Snow and Ice Data Center (http://nsidc.org/data/docs/daac/nasateam/index.html). Daily, there is a separate file for the northern and southern hemisphere. Note that the same ice data are included in a more recent netCDF product submitted to the CDR program, but the record extends only until 2007. The actual CDR which is derived from two different ice products based on the Cavalieri and the bootstrap algorithms.

3.3.2   Ancillary Inputs

All ancillary files are in IEEE format. Most are on a ¼° grid, with dimensions 1440 x 720, unless specified otherwise. Files on a 1° grid is a 360 x 180 array, while the 2° grid corresponds to a 180 X 90 array. Many ancillary files were generated by R.W. Reynolds and T. Smith using development codes not included in the submitted package.

Land/Sea Mask. This file (named quarter-mask-extend) identifies the ocean grid points to be processed (mask=1). The value is set to 0 to exclude land, permanent ice shelves, and most inland waters. The base land mask was provided by C. Gentemann (pers. comm.) and manually modified by R. W. Reynolds.

First guess. This is the OISST of the previous day. To initiate the original daily v1 runs, the weekly OISST interpolated to daily was used. For the daily OISST v2, the daily v1 was used.

Noise-to-Signal Ratio (NSR).   The OI code expects a NSR file for each of the different inputs. For ship, buoy, and ice data, the filenames are ship4sm-nsr-stat-v2, buoy4sm-nsr-stat-v2, and ice4sm-nsr-stat-v2. For AVHRR, there is a separate file for day and night, respectively named day-path4sm-nsr-stat-v2 and nte-path4sm-nsr-stat-v2 . The NSR computation is described in Reynolds and Smith (1994) and an abbreviated version is given in section 3.4.6.

Scaled Noise-to-Signal Ratio. These are similar to the NSR files except these are normalized, and the filenames have '-scaled' at the end. These are applied to data from days other than the current day.

SST climatology on 1° grid.   The file (named clim.1971.2000.dat) is the climatology for the 1971 to 2000 base period based on two intermediate climatologies: the weekly OISST v2 from 1982-2000 and an in situ climatology from 1971-2000, as explained in http://www.cpc.ncep.noaa.gov/products/predictions/30day/SSTs/explanation.html. Comparison with other 30-year periods is provided by Xue et al. (2003). Some parts of the code may use derived fields already interpolated daily for 365 and 366 days of the normal and leap years, respectively.

ICOADS standard deviation on 1° grid. The file (named stdev1-coad3-fill) contains the monthly standard deviation of ICOADS SST data from 1950 to 1979 on a 1° grid. The array is 12 x 360 x 180. It is used in screening the ship, buoy and satellite observations before forming super-observations. Gaps have been filled in by interpolation.

1° Land/Sea Mask. This mask (named lstags.onedeg.dat) is associated with the weekly OI grid. The value is set to 1 for ocean.

EOT modes on 2° grid. This file (named eot6.damp-zero.ev130.ano.dat) contains the 130 modes from Empirical Orthogonal Teleconnections analysis on a 2° grid. Gaps have been filled in by interpolation. Section 3.4.1 describes the EOT computation.

EOT variance on 2° grid. The file named var-mode contains the variance associated with each of the 130 modes.

Land/Sea Mask on a 2° grid. The file lstags.twodeg.dat contains the land/sea tags on a 2° grid and is intended for use with the EOT modes.

Residual Bias on a 2° grid. The file residual-stat-v2 contains the residual bias resulting from using only 130 modes of the total possible.

First guess variance error. The file path-incr-var-stat-v2 contains the estimated variance error of AVHRR data.

Correlation correction. The file cor4sm-stat-v2 contains the correlation correction due to the first guess.

3.3.3   Derived Inputs

The sea ice concentration data (sources specified in 3.3.1) are converted to simulated SSTs. The Grumbine sea ice concentrations are first regridded from ½° to match the ¼° OI grid. For the historic data, the separate northern and southern hemisphere maps need to be re-projected onto the rectangular grid and interpolated to fill in gaps. Both the Cavalieri and Grumbine ice fields contained single-day events when sea ice concentrations increased dramatically, especially in coastal regions. This resulted in spikes in the daily OI in areas with the sea-ice-simulated SSTs. To eliminate these issues, a 7-day median filter was applied temporally to all daily ice fields. The median smoothed sea ice data were then converted to simulated SSTs using an empirically-derived linear equation from Reynolds et al. (2007). This ice-to-SST equation is also provided in section 3.4.6 where the formulation and coefficients are also discussed.

3.3.4   Forward Models

Not applicable.

3.4   Theoretical Description

Prior to optimum interpolation (OI), a preliminary correction to the AVHRR data with respect to the in situ data must be made. This initial step is necessary because the OI method assumes that the data does not contain any long term biases. Section 3.4.1 discusses the theoretical basis of the satellite bias correction, followed by an explanation of OI. Section 3.4.2 describes Optimum Averaging (OA) which handles the merging of super-observations from different sources, prior to interpolation. The implementation of the satellite bias correction procedure and the OI is discussed in Section 3.4.4.

3.4.1   Physical and Mathematical Description

Satellite bias correction. The satellite bias correction method is based on Empirical Orthogonal Teleconnection (EOT) functions (Van den Dool et al. 2000). Reynolds et al. (2007) discusses how the EOT approach was selected instead of two other candidate methods. In brief, the EOT method was more robust on a daily scale and produced more localized spatial functions that could be tuned. Note that the EOT modes are computed only once, outside of the daily OI computations and this code package.

For a dataset $\Omega(x, t)$, that is a function of space (x) and time (t), the EOT functions are determined by finding the location with the largest spatial covariance with respect to all the other points (details in Van den Dool et al. 2000). The time series at that point is defined as $T_1(t)$. By regression, the corresponding spatial function, $X_1(x)$, is then

computed. The product of $X_1(x)$ $T_1(t)$ is subtracted from $\Omega(x, t)$ and the process is repeated. This yields a set of modes such that $\Omega(x, t) \approx \sum_{i=1}^{M} X_i(x)T_1(t)$ where M is the maximum number of modes.

Using the weekly OISST anomalies to define Ω (x, t), Smith and Reynolds (2003) determined a set of $X_i(x)$ spatial modes, where *M* was set to 130. The number of modes, M, and the spatial functions, $X_i(x)$, were determined by Smith and Reynolds (2004). The value of *M* was selected subjectively to account for most of the global anomaly variations. Because of the way the modes were selected, the higher order modes tend to be very spatially coherent. For example, the spatial scale of the 100th mode is similar to that of the first mode. The major advantage of EOTs is that modes are determined one at a time. Thus, the individual modes can be tapered so that the maximum spatial extent of the mode is limited. Smith and Reynolds (2003) used linear tapering to limit the maximum extent of their functions to 800 km to avoid large spatial teleconnections.

To avoid situations in which a mode is only sampled outside of its center of action, Smith and Reynolds (2003) defined a mode selection criteria, Ci, given by

$$C_i = \frac{\sum_x \delta(x)X_x^2\alpha(x)}{\sum_x X_x^2\alpha(x)} \tag{5}$$

where $\alpha(x)$ is the cosine weighting of the area associated with each 2° grid box. This relatively coarse grid is sufficient for the large scale bias corrections that need to be made. The Kronecker $\delta(x)$ is 1, if there are observations at grid location x, or 0, otherwise. If C_i is below a critical threshold (i.e., 15%; based on cross validation tests by Smith and Reynolds, 2003), the data are considered to be inadequate and the mode is not used. The modes that satisfy this critical sampling test are used and are fit to in situ SST data as described in Smith et al. (1996) to define the anomalies; otherwise, the modes are not used. The bias correction implementation is described in 3.4.4

Optimum interpolation. The material presented here is from Reynolds et al. (2007) and discussed in greater detail in Reynolds and Smith (1994). The OI analysis is performed on a regular grid using irregularly spaced data. The analysis is formed by a weighted sum of the input data, using the OI linear weights, w_{ik}, determined by regression. The indices *i* and *j* represent data type while *k* represents analysis grid points. The relationship can be expressed as

$$r_k = \sum_{i=1}^{N} w_{ik}q_i \tag{6}$$

where q_i are the SST data values from different sources, *N* is the number of data values, and r_k is the analyzed SST. Normally *q* and *r* are differences from a first-guess reference system, which is defined here as the analyzed SST from the previous time step. Thus, in the daily OI, *q* and *r* are the SST data and analysis increments, defined as the difference from the analysis at the previous day.

Following Reynolds and Smith (1994), it is assumed that the ensemble average of the analysis correlation error $\langle \pi_i \pi_j \rangle$ is Gaussian, such that

$$\langle \pi_i \pi_j \rangle = \exp\left[\frac{-(x_i - x_j)^2}{\lambda_x^2} + \frac{-(y_i - y_j)^2}{\lambda_y^2} \right] ,$$

(7)

where the variables x and y are the zonal and meridional data and analysis locations, and λ_x and λ_y are the zonal and meridional spatial scales (see section 3.4.6 and Table 2 for values used in the OI). The weights can then be defined by

$$\sum_{i=1}^{N} (\langle \pi_i \pi_j \rangle + \varepsilon_i^2 \delta_{ij}) w_{ik} = \langle \pi_j \pi_k \rangle ,$$

(8)

where ε_i is the noise-to-signal standard deviation ratio (see section 3.4.6). The ensemble averages of the data errors are assumed uncorrelated between different observations. Thus, the data correlation error is $\delta_{ij} = 1$ for $i = j$ and $\delta_{ij} = 0$, otherwise.

It is important to note that the actual SSTs (data and analysis) only appear in (6). The remaining equations to determine the weights depend only on the distance via (7) and noise-to-signal ratios (computation explained in 3.4.6) for the available SST data. For each analysis grid point, ε_i, λ_x, and λ_y are assumed locally constant and the set of equations are solved to determine the weights and the analyzed SST, r_k. Spatial functions are defined for each of these quantities with different fields of ε_i for each type of data. Presently, the data types are ships, buoys, SST simulated from sea ice, and day and night satellite data from the AVHRR instrument. For each of these data types, supero-bservations must first be formed to facilitate solving the equations, as explained in 3.4.4.

Once formed and bias adjusted, all super-observation types within a box are combined. The combination is carried out using a simplified optimum averaging technique (Kagan 1979), described in section 3.4.2. The assumption is that the local error correlations within each box can be approximated as 1. The OA method performs an optimal combination of all superobservations values, q_i, and the super noise-to- signal ratios, ε_i, within a grid box to form a combined observation and reduced combined noise-to-signal ratio. The combined observations and noise-to-signal ratios are the variables actually used in (5)–(7). Thus the OISST method is actually a two-step process, an OA followed by an OI, which approximates an OI-only procedure. The two-step process is computationally more efficient.

3.4.2   Data Merging Strategy

This section is derived from Appendix B in Reynolds et al (2007). Simplified optimum averaging (OA; Kagan 1979) is appropriate for combining observations of different types, and also for computing the error estimate of the combination. To begin, equation 3.3.2 in Kagan (1979) is used and rewritten here as

$$\sum_{i=1}^{n} w_i C_{ij} + w_j E_j^2 = C_{jA} \qquad , j=1,....,n$$

(9)

where C_{ij} is the covariance between observations i and j, C_{jA} is the covariance between observation j and the average value A, and E_j^2 is the noise error variance of observation j. The OA weights for the n observations are w_j.

Here the averaging region is assumed to be the OI analysis $1/4°$ spatial box. For this box it is assumed that the averaging region is small enough that all correlations within the region are equal to 1 and that the variance, σ^2, is constant within the region. With these assumptions, the OA weights for the n individual observations are found by solving

$$\varepsilon_j^2 w_j + \sum_{i=1}^n w_i = 1 \quad , j=1,...., n \tag{10}$$

where $\varepsilon_j^2 = E_j^2/\sigma^2$ is the noise-to-signal variance ratio of observation j. From (10) the weights can be expressed as

$$w_j = \frac{1-\sum_{i=1}^n w_i}{\varepsilon_j^2}. \tag{11}$$

The sum of the weights is then

$$n\overline{w} = \sum_{i=1}^n w_i = (1 - n\overline{w}) \sum_{j=1}^n 1 \Big/ \varepsilon_j^2 . \tag{12}$$

Defining $H = \sum_{i=1}^n 1 \Big/ \varepsilon_i^2$, then by algebraic manipulation of (12), the sum of the weights as a function of the normalized error variances becomes

$$n\overline{w} = \frac{H}{1+H} \tag{13}$$

and the weights are then defined as $w_j - \frac{1}{(1+H)\varepsilon_j^2}.$

Using these same assumptions, the combined noise-to-signal variance ratio is

$$\varepsilon_0^2 = 1 - n\overline{w} - \frac{H}{1+H}. \tag{14}$$

Note that these OA weights may cause damping of the solution in situations when the noise is large. To avoid this damping, the weights can be normalized, giving the solution

$$q_i = \frac{1}{H\varepsilon_i^2}. \tag{15}$$

Here the sum of the normalized weights, q_i, is equal to 1. Using Kagan's Eq. (3.3.10), it can be shown that the error using normalized weights is

$$\varepsilon_q^2 = \varepsilon_0^2 + \frac{(1-n\overline{w})^2}{n\overline{w}} = \frac{1}{H}. \tag{16}$$

Note that this error reduces to the error from (14) as the sum of the weights approaches 1. Otherwise it is slightly larger. The normalization has been implemented in the current OI SST processing.

3.4.3   Numerical Strategy

The forming of super-observations is a key strategy for the OI computation. The set of linear equations defined by (8) is then solved only at each OI grid point, k. To reduce computing time, only data points near the analyzed grid point are used. This approach is reasonable because (7) approaches zero with increasing data-to-gridpoint distance. Also, the solution of the set of linear equations becomes more difficult to solve when data points approach each other because the rows defining $\langle \pi_i \pi_j \rangle + \varepsilon_i^2 \delta_{ij}$ become closer to each other, leading to a degenerate solution (i.e., the determinant approaches zero). To avoid this possibility, each type of observation within a grid box is first averaged into a superobservation for the grid box, which is assumed to be at the center of the box.

3.4.4   Calculations

The calculations described here are the satellite bias correction (zonal and EOT-based), the OI, and the error. The preparation of the in situ data and ice proxy SSTs have been described in previous section 3.3.

Zonal Bias corrections. Reynolds et al. (2002) found that the Pathfinder AVHRR SSTs have cold biases with respect to operational Navy AVHRR. Reynolds (2008) showed that the Navy and pathfinder bias corrections have a residual, long-term difference possibly due to cloud Pathfinder contamination in the Intertropical Convergence Zone, and high latitude differences where in situ data are sparse. As a correction, smoothed zonal in situ minus satellite differences, $z(y)$, were computed directly from the data. These differences were subtracted from the satellite data (before the bias correction based on EOTs) and then added back onto the biases. Note that this zonal correction has no net impact on the bias correction unless there are no EOT modes. In that case the $B(x,y) = z(y)$. The zonal correction tends to reduce the difference between 60°S and 40°S, and has little impact outside of the region even at high Northern latitudes. Although there are differences at high latitudes which are not corrected by the EOT method, the biases are not zonal between 70°N and 80°N so $z(y)$ is small there.

Bias Correction based on in situ data. The pre-calculated 130 EOT spatial modes (explained in 3.4.1) are used for the bias adjustment (relative to in situ data) of each satellite dataset. Note that the number of days of data used for this step was increased from 7 days (in v1) to 15 days (in v2) to reduce noise, particularly in the pre-1990 El Nino Index (Reynolds 2008). The 15 days (current day ± 7 days) of in situ data and satellite data are converted into anomalies and then separately averaged onto a 2° grid. Modes are determined for each of the 15 days, separately for daytime and nighttime. Each time, it is important to select the same modes for both in situ and satellite. Thus, modes were only selected if C_i, defined in (5), for both sets was greater than 15%. Modes centered on the Southern Ocean, an area with little or no in situ data, was represented by the satellite data but not by the in situ data, and therefore were rarely selected (Reynolds et al. 2007). If no EOT modes are selected, the zonal adjustment described in the prior paragraph will be used. The temporal factors are also determined for the EOT modes used for each set of anomalies. The difference between the two reconstructed EOT fitted fields (satellite minus

in situ) is then computed as the bias adjustment. However, prior to use, the mode weights are first temporally smoothed using a 5-day binomial filter. This minimizes jumps in the biases that can occur as time changes and data either appears or disappears from the 15-day window. The smoothed adjustment is then interpolated from 2° to the 1/4° grid and used to correct each satellite super-observation. The correction method is applied separately for day and night and for each satellite instrument. The corrected satellite super-observations are then ready for the two-step OI.

Optimum Interpolation. To solve (8), a box centered on each grid point is defined that contains all the observations to be used for that grid point. Recall that to prepare for the OI, all types of super-observations within the 1/4° grid box are combined by OA (section 3.4.2). Thus, *N* is not only the number of superobservations; *N* is also the number of grid boxes with data. The box size is defined to be R_{max} and the maximum number of superobservations is limited to a specified value of *N*, N_{max}. Next, rough weights were computed for the special case where off- diagonal elements in (8) were zero. In that case, the rough weights would be

$$w_{jk} = \frac{\langle \pi_j \pi_k \rangle}{(1+\varepsilon_i^2)}. \tag{17}$$

The rough weights are ordered by decreasing magnitude and only data points corresponding to the largest ones were selected such that $N \leq N_{max}$. The algorithm to solve (8) includes a parameter to show when the determinate is close to zero. In that case, N_{max} is reduced for that grid point and a reduced set of observations is selected using the ordered rough weights. For the daily OI, R_{max} was set to 400 km and N_{max} to 22.

Error estimates. The error reported in the final product is the combination of two error estimates. Here, the OI random and sampling error is discussed first, followed by the bias error. The OI random and sampling error, E_k^2, can be computed (the bias error is described in the next subsection) following Reynolds and Smith (1994)

$$E_k^2 = V_k^2 (1 - w_{ik} \langle \pi_i \pi_j \rangle) \tag{18}$$

where V_k^2 is the AVHRR OI analysis increment variance. Note that the equivalent equation in Reynolds and Smith (1994) contains a typographical error in the last subscript. The expected random and sampling error defined by (6) reduces V_k^2 by the observations used in the OI. The standard deviation, V_k, is largest in western boundary current regions where mesoscale eddies are common, and smallest in the subtropical convergence areas and at high latitudes.

The EOT bias adjustment method has the additional important advantage that it can be used to define an estimate of the bias error. This is done by assuming that the satellite bias error is related to satellite EOT modes which could not be corrected by the in situ data plus a residual. The individual EOT bias variance, E_{Bj}^2, is

$$E_{Bj}^2 = \sum_{i=1}^{M} \Delta_{ij} X_i^2(x)\, \sigma_i^2 \tag{19}$$

where j is an index for the number of satellite sources used. The factor Δ_{ij} is 1 if the mode was not adequately sampled by either the satellite or the in situ data; otherwise, it is 0. The bias variance associated with each mode is σ_i^2, which was estimated by computing the satellite reconstructed anomaly modes for 1985–2005 and then determining the variance of each mode. The anomaly variance was found to be similar to the bias variance for those modes adequately sampled, allowing the bias variance of those modes to be computed. The values of σ_i^2 generally decrease with increasing value of the index i. Equation (19) is probably an overestimate of the EOT bias error because the modes are almost, but not completely, orthogonal. Thus, the non-orthogonal overlap of modes can count the variance in some regions more than once, giving an overestimate.

The total bias error E_B^2 can be expressed as

$$E_B^2 = E_{B0}^2 + \frac{1}{mn}\sum_{i=1}^{M} E_{Bj}^2 \tag{20}$$

where n is the total number of sets of satellite data used for which biases are estimated by (19), m is the number of independent satellite instruments, and E_{B0}^2 is the residual error variance for the bias not resolved by the modes. The value of E_{B0}^2 was set equal to 0.01°C^2. This value was estimated by examining residual differences between AMSR and AVHRR and by the residual difference between ships and buoys.

In (19), day and night observations from the same satellite have been assumed to be dependent data, while observations from different satellite are independent. Thus, if just AVHRR day and AVHRR night are used, m=1 and n=2, and E_{Bj}^2 from the two satellite sources is simply averaged. If more than one AVHRR instrument is used, then n= 4. If day and night data from a different sensor (e.g., AMSR) were used, then m=2, n=4, and E_{Bj}^2 from all four satellite sources is averaged and then divided by 2. In this case the average bias is reduced because two independent satellite sources are used. Note that the modes defined by Δ_{ij} in (19) may be different at the same time step because the satellite data distribution can vary even though the in situ distribution is the same. However, for the 15-day period used for the bias adjustment, all modes can usually be expressed by the satellite data alone; thus, Δ_{ij} is usually the same.

The total error variance assumes that the random and sampling error and the bias error are independent and is therefore simply the sum of E^2 from (6) and E_B^2 from (9) at each grid point. The total error reported in the netCDF file is the square root of this sum, and therefore is a standard deviation with units in °C. As noted by Reynolds et al (2007), this total error has large scale patterns south of 40°S primarily due to limited in situ data. The bias errors decrease when data from two independent satellite instruments are used (e.g., the AVHRR+AMSR product). The random and sampling errors are higher in regions between the satellite swaths. In the regions with data, the random and sampling errors are very small because of the dense satellite coverage. The sampling and random errors are even lower when AMSR is added to AVHRR data.

3.4.5   Look-Up Table Description

Not applicable*.*

3.4.6   Parameterization

Ship SST bias correction. Before the late 1990s, there were very few buoy observations, and ships were the primary source of in situ SST data. The buoy spatial coverage then increased with time while ship coverage decreased (Reynolds et al 2002). The random and bias error of ship SSTs are larger than those of buoy SSTs (Reynolds et al. 2007), and needs to be accounted for as the contribution from ships and buoys changed. Monthly averaged ship biases were computed with respect to buoys to determine the variability of a globally averaged bias. However, even with temporal smoothing, differences occurred at irregular intervals and did not seem to be related to seasonal or ENSO events. Figure A1 in Reynolds et al. (2010) shows monthly scatter plots of the collocated average global ship and buoy anomaly SSTs for two 9-year period. The average fitted intercept was -0.13°C, but the buoy minus ship difference was found to be -0.14°C when the average global difference was computed directly. This 0.01°C difference is not significant, so 0.14°C used for the ship bias adjustment, i.e., this constant was subtracted from all ship superobservations before they are used in the satellite bias correction and in the OI analysis.

Coefficients for Ice-to-SST equation. For the conversion of ice concentrations to SST, a linear formulation was preferred over a quadratic, primarily because the quadratic fit was more unstable at low ice concentrations (details in Appendix A in Reynolds et al. 2007). The linear equation is:

$$T_I = bI + c, I <= I_0 \qquad\qquad (21)$$

where T_I is the simulated SST, I is the ice concentration fraction, which varies from 0 (0%) to 1 (100%), and I_0 is the minimum value of I used to simulate SSTs. The coefficients b and c were determined by a climatological least squares fitting procedure using collocated data (AVHRR and in situ) and sea ice concentrations. The regression was performed for 30° wide longitude bands (or sectors) for the Northern and Southern Hemispheres. In addition, there were separate 30° wide bands for the North Pacific south of 66° N, and one each for the Baltic Sea and Great Lakes. These extra regions were necessary because the sea ice in these regions behaves differently than the rest of the corresponding Northern hemisphere band. The coefficients are assumed to be locally constant by month and by region. For both equations the coefficients are constrained so that T_I is equal to the freezing point of water (-1.8°C for seawater and 0°C for freshwater, i.e. Great Lakes) for ice concentrations of $I = 1$.

The value of I_0 was determined to be 0.5 based on a test using a 10-year dependent period for training and an independent 10-year period for validation. The coefficients for the linear ice-to-SST algorithm were determined for the dependent period, and then, the equation was evaluated by examining the rms and bias differences between the simulated and actual SSTs for the validation period. The rms differences were found to increase with decreasing ice concentration, particularly below 0.5. For this reason, the OI is allowed to fill in the values when I is 0.5 or less, rather than simulating SSTs where rms

differences were large. Thus, SSTs were simulated from ice concentrations for I > 0.5 and no SSTs were simulated for I ≤ 0.5. For actual use in the daily OI, the coefficients were recomputed for the entire 20-yr period (1985–2004).

      Reynolds et al. (2007) noted that when sea ice was present in the Great Lakes in 2003, the linear ice-to-SST algorithm produced unrealistic (about -18°C) anomalies in Lake Ontario. D. J. Cavalieri (2006, personal communication) explained that algorithms used to obtain sea ice concentrations from satellite data were not designed for low salinity water. Therefore, the ice-derived SSTs are not used in the Great Lakes or the Baltic Sea. Since sea ice concentrations are not produced regularly for the Caspian Sea, no ice-simulated SSTs are generated there either.

      Spatial Correlation scales and noise-to-signal ratios. The spatial correlation scales and NSR are computed for each data type, outside of the submitted OISST code. These scales are specific to the first-guess reference system used (in this case, the previous day's analysis) to define q and r in the OI equation (6). Following Reynolds and Smith (1994), spatial lagged correlations were computed zonally and meridionally for each grid point. Fitting procedures yield average λ_x and λ_y for AVHRR (or AMSR), and ε for each type of data, i.e., ice proxy SST, ship, buoy, satellite. For operational AVHRR, the day and night algorithms are different. However, the day and night algorithms are the same for Pathfinder AVHRR (and AMSR), and thus the same value of ε were used for both day and night.

Table 2: Correlation scales (λ) and Signal-to-noise (ε) used in the ¼° Daily OISST are different from the Weekly OISST

Variable	Data type	Weekly OI.v1	Weekly OI.v2	¼° Daily OI.v1 and v2
λ	ship	3.90		1.94
	buoy	1.50		0.50
	ice	1.00		0.50
	AVHRR day	1.46		0.50
	AVHRR night	0.88		0.50
ε	Zonal (λ_x)	859 km	850 km	151 km
	Meridional (λ_y)	608 km	615 km	155 km

      The results of these statistical estimates are summarized in terms of average values (60°S–60°N) for both the weekly OI and the OISST (Table 2). The NSR are much smaller for the daily OI than the weekly OI, thereby allowing much finer spatial resolution of the SST field. Note that in Table 1, the overall zonal and meridional scales for the weekly OI are quite different, while those for QDOISST scales are very similar. However, the QDOISST scales do vary geographically: they are larger in the Tropics (150–200 km) than at higher latitudes (100–150 km) and smallest (50–100 km) primarily in the regions of western boundary currents. Examples of the impact of λ is given in Reynolds et al. (2008).

The choice of the spatial error scales, λ, partially determines the spatial smoothing. If λ is equal to the size of the grid box, then each grid box is analyzed independently. This would make the analysis very noisy because many grid boxes would have no data (unless microwave data, which has quasi all weather coverage, were used). However, if λ were very large (e.g., 1000 km) many of the finer gradient details would be reduced, as in the weekly OI.

3.4.7   Algorithm Output

The primary output is the analyzed SST, and the file contents and units have been described in section 2.1. The netCDF filename is avhrr-only-v2.yyyymmdd.nc where yyyymmdd is the date. The compressed (gzip) files are typically 1.8 megabytes and can be downloaded from ftp://eclipse.ncdc.noaa.gov/pub/OI-daily-v2/NetCDF/yyyy/AVHRR/ where yyyy is the 4 character year.

4.   Test Datasets and Outputs

4.1   Test Input Datasets

None.

4.2   Test Output Analysis

4.2.1   Reproducibility

None.

4.2.2   Precision and Accuracy

There are no absolute sea truth data to determine precision. To evaluate precision and accuracy, it is not recommended to compare against in situ data, which are blended into the analysis. Obviously the two are not independent and good agreement is expected. The product may be compared against Argo buoy data which are withheld from the analysis exactly for the purpose of validation. However, Argo buoy data were not collected until recent years and cannot be used for the early part of the time series. Also, the OISST may be compared against different single sensors (e.g., MODIS, VIIRS, AMSR) although this may tend to reveal more about the sensor than the analysis.

4.2.3   Error Budget

As discussed in section 3.4.4, the total error provided is comprised of the bias, random and sampling error. This is computed each time the analysis is performed, for each gridpoint.

5.   Practical Considerations

5.1   Numerical Computation Considerations

The algorithm is implemented from research code, with no attempt at parallelization. This analysis is designed to be performed serially, since each day is initialized by the previous day's result. In theory, if the analysis is started using a dummy field (such as the weekly OI or the previous v1 daily OISST), the results will be fairly stable after a few weeks. For this reason, it is recommended to use the daily OISST no earlier than November 1981.

5.2   Programming and Procedural Considerations

Not applicable.

5.3   Quality Assessment and Diagnostics

Plots of the OISST are made daily for visual checks. The OISST may also be compared against other SST analyses (also known as Level 4 SSTs). NOAA/STAR has a website tool called the SST quality monitor (SQUAM) that performs this task (http://www.star.nesdis.noaa.gov/sod/sst/squam/index.html).   If any large departure from other analyses occurs, it would need to be investigated. The daily ¼ ° OISST is one of the SST analyses that comprise the GHRSST Multi-Product Ensemble (GMPE), available at http://ghrsst-pp.metoffice.com/pages/latest_analysis/sst_monitor/daily/ens/index.html. The difference between the daily OISST and GMPE is shown by selecting "NOAA AVHRR OI minus ensemble median" and the date.

The most common problem is with input data, which may be missing or have reduced coverage. For consistency over decades, it would be best to have the capability to make time series plots, globally or locally of differences with respect to a set of references. Plots of latitudinal band averages over time, also known as Hovmöller (1949) diagrams, are excellent tools.

5.4   Exception Handling

To be discussed in detail in the Operation Algorithm Description (OAD)", which will be CDRP-OAD-0301.

5.5   Algorithm Validation

Reynolds et al (2007) compared the daily OISST against analyses using the same code base but with input of only satellite data, in situ data only, with and without bias correction. Reynolds et al (2007) also made detailed comparisons against some other SST analyses produced elsewhere. It should be borne in mind that all existing SST products continue to be updated, revised and reprocessed, so some of the information in Reynolds et al (2007) may be no longer apply to the more recent product versions. More recent

comparisons among GHRSST SST analyses can be found in Dash et al (2012) and Martin et al (2012).

5.6   Processing Environment and Resources

The operational run is performed on a Linux machine (Intel hardware) with the Centos 5.9 operating system. The programming code is in Fortran77 and Fortran90, and executables are generated using the Lahey Fortran 6.20a compiler using the netCDF library 3.6.0.

Daily cron jobs run shell scripts that control all the processing from data download to netCDF conversion to plotting of the output. To read NCEP ice data, wgrib2 functions (http://www.cpc.ncep.noaa.gov/products/wesley/wgrib2/) are used. Plots are made using GRADS 2.0.2 (http://grads.iges.org/grads/grads.html). The plots are used for quality control and are posted at the OISST website.

For the preliminary (1-day delay) run, a single day analysis uses a total CPU of about 1 minute (40 sec) and wall clock time of about 2 minutes. For the final (15-day delay) product, the run time uses about the same total CPU as the preliminary and 1 minute wall clock time. About 0.4 Gb of space is needed to run one day. This takes into account space for input, intermediate and output files. There is no dynamic memory allocation required.

6.   Assumptions and Limitations

6.1   Algorithm Performance

The analysis is limited by the data coverage. Analysis results will be degraded where there are no SST observations, particularly if there are big gaps in space and/or time. The bias correction is dependent on in situ data, and therefore not very reliable where there is no in situ data (especially near polar regions).

6.2   Sensor Performance

Assumptions about the sensors are made by the input data providers, who apply their algorithms to provide SSTs and ice concentrations. For the OI, it is assumed that all AVHRRs from 1981 to the present have the same statistical characteristics, e.g., noise-to-signal ratio. Note that the microwave instruments such as AMSR-E have very different statistical characteristics from AVHRR.

7.   Future Enhancements

7.1   Enhancement 1: reprocessing

OISST needs to be re-run with updated climate quality datasets that continue to be extended and revised. For example, PFSST5.2 is now available up to 2011 in netCDF4, not HDF, and at ~4.6 rather than 4.9 km resolution. The delayed-mode NASA Team sea ice concentrations are available up to 2010, and a near real time version is also produced with 1-day delay. It would be more consistent to use this instead of the Grumbine product. A new 30 year climatology based on the current daily OISSTv2 can replace the old one based on the weekly OI. The ICOADS dataset has also been updated to release2.5 and a new release is expected at the end of 2014.

7.2   Enhancement 2: new satellites

The code is not set up to accept any generic satellite. As sensors are retired, the code must be modified to accommodate new satellites. In particular, the last AVHRR will be flown on METOP B. The official NESDIS product, which will be archived in CLASS, will use the Advanced Clear Sky Processor (ACSPO) algorithm developed by NOAA/STAR, and the file format and resolution will most likely be different. The Navy will continue to produce SSTs in the heritage format and resolution but the data has to be obtained directly from the Navy and will not be automatically archived in CLASS. SST data from VIIRS and future infrared sensors can be used but the "AVHRR-only" label has to be changed.

7.3   Enhancement 3: infrared+microwave resurrection

Related to Enhancement 1 is the continuation of the AMSR+AVHRR series using AMSR2 SSTs, and bridging the gap using WindSat. Microwave coverage is superior to AVHRR and therefore provides more accurate SST fields in the open ocean. AVHRR remains essential for coastal coverage. The AMSR data used in the existing product was produced by Remote Sensing Systems with their version 5 algorithm. Now, the AMSR data has been updated to version 7 and WindSat is available only as version 7. As mentioned previously, PFSSTv5.2 is now available. The product also has to be renamed since WindSat instrument has a very different design and viewing geometry compared to AMSR.

7.4   Enhancement 4: night-like OI

The daily OI combines daytime and nighttime observations, and therefore contains a diurnal warming contribution that is ambiguous and variable in space in time. Satellites observe different phases of the daily heating cycle depending on the overpass time. To examine climate trends, it is desirable to minimize the variability introduced by this daily heating. Therefore a night-like SST analysis would be useful. Ideally, this product would use only nighttime satellite data, but the reduced amount of input data introduces a different variability into the OI. One possibility is to add wind-screened daytime data, or to adjust the fields to a pre-dawn time (e.g., 2:30 am) using a simply diurnal model. The night-like temperature would also be a good starting point for producing sub-daily SSTs.

7.5   Enhancement 5: high resolution analysis

Reynolds and Chelton (2013) describe a two stage OI analysis that uses the ¼° AVHRR+AMSR and then performs a second interpolation at a higher resolution (1/24°) wherever there is AVHRR data. This product could be very useful for feature-tracking or local scale applications including air-sea interaction studies, fisheries and resource management.

8.   References

Banzon, Viva F., Richard W. Reynolds, 2013: Use of WindSat to Extend a Microwave-Based Daily Optimum Interpolation Sea Surface Temperature Time Series. J. Climate, 26, 2557–2562. doi: http://dx.doi.org/10.1175/JCLI-D-12-00628.1

Cavalieri, D. J., C. L. Parkinson, P. Gloersen, J. C. Comiso, and H. J. Zwally, 1999: Deriving long-term time series of sea ice cover from satellite passive-microwave multisensor data sets.J. Geophys. Res., 104, 15 803–15 814.

Dash, P., and Coauthors, 2012: Group for High Resolution Sea Surface Temperature (GHRSST) analysis fields inter-comparisons-Part 2: Near real time web-based level 4 SST Quality Monitor (L4-SQUAM). Deep-Sea Research Part Ii-Topical Studies in Oceanography, 77-80, 31-43

Grumbine, R. W., 1996: Automated passive microwave sea ice concentration analysis at NCEP. NOAA Tech. Note 120, 13 pp. [Available from NCEP/NWS/NOAA, 5200 Auth Road, Camp Springs, MD 20746.]

Hovmöller, E., 1949: The Trough-and-Ridge Diagram, Tellus 1 (2): 62–66.

Kagan, R. L., 1979: Averaging of Meteorological Fields. Gidrometeoizdat, 212 pp. (Translated from Russian by L. S. Gandin and T. M. Smith, Eds., Kluwer Academic, 1997.)

Kilpatrick, K. A., G. P. Podesta, and R. Evans, 2001: Overview of the NOAA/NASA advanced very high resolution radiometer Pathfinder algorithm for sea surface temperature and associated matchup database. J. Geophys. Res., 106, 9179–9198.

Martin, M., and Coauthors, 2012: Group for High Resolution Sea Surface temperature (GHRSST) analysis fields inter-comparisons. Part 1: A GHRSST multi-product ensemble (GMPE). Deep-Sea Research Part Ii-Topical Studies in Oceanography, 77-80, 21-30.

May, D. A., M. M. Parmeter, D. S. Olszewski, and B. D. McKenzie, 1998: Operational processing of satellite sea surface temperature retrievals at the Naval Oceanographic Office. Bull. Amer. Meteor. Soc., 79, 397–407.

Reynolds, R.W., C. L. Gentemann and G. K. Corlett, 2010: Evaluation of AATSR and TMI Satellite SST Data. J. Climate, 23, 152-165.

Reynolds, R. W., T. M. Smith, C. Liu, D. B. Chelton, K. S. Casey and M. G. Schlax, 2007: Daily High-resolution Blended Analyses for sea surface temperature. J. Climate, 20, 5473-5496.

Reynolds, R. W., N. A. Rayner, T. M. Smith, D. C. Stokes, and W. Wang, 2002: An improved in situ and satellite SST analysis for climate. J. Climate, 15, 1609–1625.

Reynolds, R. W. and T. M. Smith, 1994: Improved global sea surface temperature analyses. J. Climate, 7, 929-948.

Smith, T. M., and R. W. Reynolds, 2003: Extended reconstructionof global sea surface temperatures based on COADS data (1854–1997). J. Climate, 16, 1495–1510.

Smith, T. M., and R. W. Reynolds, 2004: Improved extended reconstruction of SST.J. Climate, 17, 2466–2477

Van den Dool, H. M., S. Saha, and Å. Johansson, 2000: Empiricalorthogonal teleconnections. J. Climate, 13, 1421–1435.

Worley, S. J., S. D. Woodruff, R. W. Reynolds, S. J. Lubker, and N. Lott, 2005: ICOADS release 2.1 data and products. Int. J. Climatol., 25, 823–842.

Xue, Y., T. M. Smith, and R. W. Reynolds, 2003: Interdecadal changes of 30-yr SST normals during 1871–2000. J. Climate,16, 1601–1612.

Appendix A.   Acronyms and Abbreviations

Acronym or Abbreviation	Meaning
ACSPO	Advanced Clear Sky Processor
AMSR	Advanced microwave Scanning Radiometer
AMSR-E	AMSR on the EOS platform
AVHRR	Advanced very High Resolution Radiometer
C-ATBD	Climate Algorithm Theoretical Basis Document
CDR	Climate Data Record
DMSP	Defense meteorological Satellite Program
EOS	Earth Observing System
Fortran	FORmula TRANslating system
GHRSST	Group for High Resolution SST
GMPE	GHRSST Multi-product Ensemble
GRIB	General Regularly-distributed Information in Binary form
GTS	Global Telecommunications System
HDF	Hierarchical Data Format
ICOADS	International Comprehensive Ocean-Atmosphere Dataset
IEEE	Institute of Electrical and Electronics Engineers
METOP	Meteorological Operation satellites
NASA	National Aeronautic and Space Administration
NCDC	National Climatic Data Center (NOAA)
NCEP	National Centers for Environmental Prediction (NOAA)
NESDIS	National Environmental Satellite, Data Information Service
netCDF	Network Common Data Form
NOAA	National Oceanic and Atmospheric Administration
NODC	National Oceanographic Data Center (NOAA)
NSIDC	National Snow and ice Data center
NSR	Noise-to-Signal Ratio
OA	Optimum Averaging
OI	Optimum Interpolation
OISST	Optimum Interpolation Sea Surface Temperature
PFSST	Pathfinder SST
PODUG	Polar Orbiter Data Users' Guide
SQUAM	SST Quality Monitor

SST	Sea Surface Temperature
SSMI	Special Sensor Microwave Imager
SSMIS	Special Sensor Microwave Imager Sounder
SSMR	Special Sensor Microwave Radiometer
STAR	Center for Satellite Applications and Research (NOAA)